Synthesis and characterization of $Gd_{0.1}Ce_{0.9}O_{1.95}$ nanopowder via an acetic–acrylic method

Ai Zhu Liu, Jian Xin Wang, Chang Rong He, He Miao, Yi Zhang, Wei Guo Wang[*]

Division of Fuel cell and Energy Technology, Ningbo Institute of Material Technology & Engineering, Chinese Academy of Sciences, Ningbo 315201, PR China

Abstract

Nanocrystalline $Ce_{0.9}Gd_{0.1}O_{1.95}$ (GDC) powders are successfully prepared by an acetic–acrylic method using acrylic acid, cerium acetate and gadolinium acetate as the starting materials. The polymeric precursors are characterized by means of TG/DTA, XRD and FT-IR, and the resultant powders are characterized by XRF, BET, SEM and particle size distribution (PSD) analysis. It is shown that the morphology of the oxide particles is dependent on the preparation conditions such as molar ratio of acrylic acid to metallic ions (L/M) and the sort of surfactant. High purity, single phase, homogeneous, nanocrystalline GDC powders with slight aggregation are obtained using ethylene glycol as surfactant, $L/M = 0.5$ and heat treatment above 600 °C. The low application amount and high effect of acrylic acid is attributed to the co-operation of carboxyl group and ethylenic bond. The electrical conductivity of the sintered GDC pellet is 0.053 Scm^{-1} in air at 750 °C. The present work indicates that the acetic–acrylic method is a relatively green method without any NO_x to synthesize high performance GDC powders.
© 2013 Elsevier Ltd and Techna Group S.r.l. All rights reserved.

Keywords: C. Ionic conductivity; E. Fuel cells; Acetic–acrylic synthesis; Gadolinium doped ceria

1. Introduction

Solid oxide fuel cell (SOFC) is one of the cleanest, most efficient and versatile technology for the chemical to the electrical energy conversion. Among all the oxygen ion conductors, yttria stabilized zirconia (YSZ) is the most commonly used for the SOFCs. This typical material requires a high operation temperature which leads to several technological problems, such as mechanical instability, reduced lifetime and undesirable reactions between the cell components. Doped ceria has more oxygen vacancies and it shows a higher oxide ionic conductivity than YSZ. In the rare-earth doped ceria, the highest conductivities are observed for $Ce_{1-x}Gd_xO_{2-x/2}$(GDC).

Various methods have been used to prepare nano-sized doped ceria, such as the sol–gel [1–4], microwave-combustion [5–9], acrylamide polymerization [10,11], polymer-pyrolysis [12], microemulsion [13,14], homogeneous precipitation [15,16], hydrothermal [17,18] and mechanochemical [19,20].

The most common used method is the combustion method, which starts with the metal nitrates and the citric acid. The powders prepared by the combustion method are more homogeneous, have fewer impurities and higher surface areas. Dong et al. [5] tried to induced a polymer hydrogel assisted combustion synthesis to produce highly crystalline ceramic nanoparticles using cross-linked poly-acrlyamide hydrogel as the fuel. However, during the combustion process, the volume expands and sometimes even the precursor burns. To our experience, this will make the process uncontrollable and some problems involves when it comes to scale up.

Liu et al. [12] induced a polymer-pyrolysis route to synthesize nanocrystalline materials with high yield and large scale. The simultaneously polymeric precursors were made by in situ polymerization of the mixed aqueous solution of acrylic acid in the presence of metal nitrates, with $(NH_4)_2S_2O_8$ as the initiator. They believed the metallic ions were bound by the strong ionic bonds between the metallic ions and carboxylate ions in a polymeric chain or between the polymeric chains. However, it should be mentioned that the pretreatment process in the polymer-

*[*]Corresponding author. Tel.: +86 574 87911363; fax: +86 574 87910728.
E-mail address: wgwang@nimte.ac.cn (W.G. Wang).

pyrolysis method can produce some NO_x due to the decomposition of the residual NO_3^-.

The acrylamide polymerization process in the synthesis of highly dispersed mixed oxides has been described by Sin [21]. Tarancón [11] chose nitrate salts to synthesize ultrafine and highly homogeneous powder of $Gd_{0.2}Ce_{0.8}O_{1.9}$. In this powder synthesis process, the monomers of acrylamide ($CH_2=CHCONH_2$), the initiator and the cross-linker were dissolved to form the chains of polyacrylamide. During the polymerization process, an auxiliary three-dimensional (3D) tangled network was formed by polyacrylamide gel, in a solution of the appropriate cations. They believed the complexation of cations by acrylamide significantly decreased the rate of the polymerization reaction and impeded the formation of the 3D tangled network. In order to avoid metal-complexation by acrylamide, they chelated the cation in solution by EDTA. This method can be used to synthesize ultrafine powders of a wide variety of ceramic materials with applicability in SOFC. However, it is known that the acrylamide is neurovirulence and the high toxicity level of acrylamide forced them to search for an alternative monomer for gel constitution.

In this study, we report for the first time the preparation of nanocrystalline GDC via an acetic–acrylic method without using any nitrate materials. The pyrolysis process was studied by means of TG/DTA, XRD and FT-IR. The synthesis conditions of the molar ratio of acrylic acid to metallic ions and surfactants were also optimized. Furthermore, we studied the mechanism of acrylic acid using the FT-IR spectra and SEM. The electrical property of the material was also studied by a frequency response analyzer.

2. Experimental procedure

2.1. Powder synthesis

Cerium acetate hydrate ($Ce(CH_3COO)_3 \cdot 4H_2O$, 99.99%, Aladdin) and gadolinium oxide (Gd_2O_3 99.99%, Aladdin) were used as metallic precursors. Acetic acid and acrylic acid were used as solvent and polymerized monomer in the synthesis of $Ce_{0.9}Gd_{0.1}O_{1.95}$. The synthesis of the powders by the acetic–acrylic method is shown as a flow chart in Fig. 1. A stoichiometric amount of Gd_2O_3 was dissolved in acetic acid and cerium acetate hydrate was added subsequently to obtain a mixed acetic aqueous solution. Different amounts of acrylic acid with the molar ratio of acrylic acid to metallic ions (L/M) of 0, 0.5, 1 and 4 were added to the solution respectively to study the influence on morphology. Lastly, 0.5 g of different surfactants PEG, PVA, PVP and EG were added to study its effect on the synthesis process.

The solution was heated and stirred in a water bath at the temperature of 80 °C for 5 h to evaporate the water. Then the white gel-like precursors were dried at 110 °C for 12 h and 250 °C for 6 h later. Finally, the obtained yellow ash was heated in a muffle furnace at different temperatures to investigate its properties of structure and sintering.
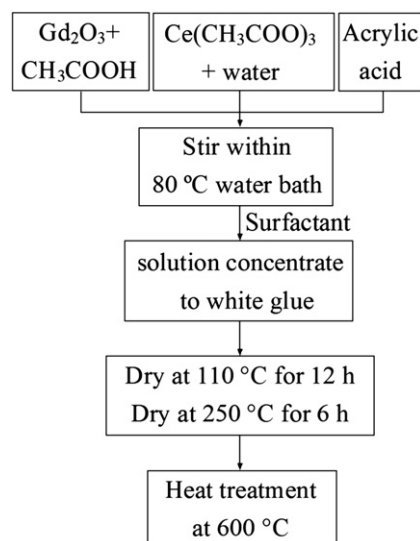

Fig. 1. Flow chart of GDC synthesis by the acetic–acrylic method.

2.2. Powder characterization

To study the thermal decomposition process and the phase evolution, the gel precursor was dried in a vacuum oven at 110 °C. TG/DTA analysis at the temperature range of 30–900 °C was carried out with a heating rate of 5 °C min^{-1} in air. The room temperature X-ray powder diffraction (XRD) data were collected on a diffractometer with Cu-Kα radiation. Data were recorded at a step of 0.02° s^{-1} in the range of 2θ from 10° to 90°. The structural feature of the polymeric GDC precursor and reactants were characterized by Perkin-Elmer FT-IR spectroscopy using KBr pellet method in the range of 500–4000 cm^{-1}. The purity of the synthesized GDC powders was measured by XRF (Rigaku ZSX Primus II). Specific surface areas of GDC powders were measured by the Brunauer Emmett Teller (BET) isotherm technique with nitrogen adsorption using a Micromeritics ASAP 2020M physisorption analyzer. Particle size distribution (PSD) analysis was made by Zatasizer Nano ZS Malvern Instruments Ltd. (UK). The morphologies of the synthesized powders and pellets were characterized by means of scanning electron microscopy (SEM) using a Hitachi S-4800 microscope.

The resultant GDC powders were pressed into a pellet of 8 mm diameter and 1.0 mm thickness under a pressure of 300 MPa, and then sintered at 1500 °C for 5 h. The impedance was measured using a frequency response analyzer (Soltron 1260) over a frequency range from 0.1 Hz to 10 MHz at 400–800 °C in air. The ionic conductivity σ and the activation energy E_a were derived from the impedance data.

3. Results and discussion

To study the chemical reactions of the gel precursor occurred in the pyrolysis process, TG/DTA, FT-IR, and XRD analysis of the precursor were conducted. The TG/DTA results of the GDC precursors dried in a vacuum
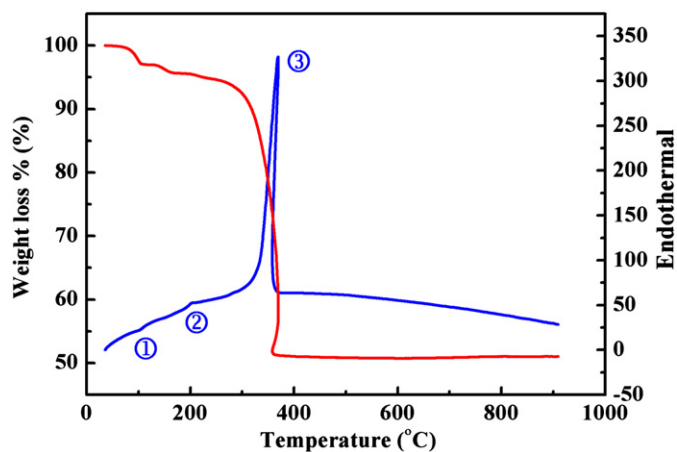
Fig. 2. TG/DTA curves of GDC precursor dried at 30 °C.

Fig. 3. XRD patterns of GDC powders calcined at 400, 600, 800 and 1500 °C, respectively ($L/M=0.5$).

oven at 110 °C are presented in Fig. 2. The total weight loss was 49.3% and most of it occurred between 250 and 400 °C. In the TG curve, three main weight loss domains are observed in temperature ranges: 60–150, 150–250 and 250–400 °C. The first domain corresponds to the endothermic peak at 105 °C in the DTA curve and it is assigned to the loss of moisture and the dehydration of acetate. The next domain is due to the decomposition of the polyacrylic which is related to the exothermic peak at 200 °C in the DTA curve. The sharp and strong exothermic peak at 366 °C might be resulted from the oxidation of the acetate. The steep weight loss of 42% at this stage might be related to the burn-out of the residual organic compounds. The decomposition of the acetate produced CO_2 and H_2O without any NO_x, which is more environmental friendly compared to the polymer pyrolysis method [12]. Beyond 400 °C, there is neither weight loss nor reaction, which indicates the formation of the $Ce_{0.9}Gd_{0.1}O_{1.95}$ phase.

The precursors treated at different temperatures show main reflections of cubic fluorite structure of GDC without any residual impurities. XRD patterns for the GDC powders sintered at 400, 600, 800 and 1500 °C respectively are shown in Fig. 3. It can be seen that the single fluorite phase is nearly formed after heat treatment at 400 °C for 5 h. This is in good agreement with the TG/DTA results that the whole pyrolysis process was completed below 400 °C. The XRD patterns become sharper with the increasing calcination temperature, indicating the gradual growth of the crystallite size of the GDC powder. According to the Debye-Scherrer Formulation, the simulate grain size of the particle at 400 °C, 600 °C and 800 °C is 6.4 nm, 16.5 nm and 42.4 nm, respectively. The pattern of the pellet calcined at 1500 °C remains the cubic fluorite structure also, indicating the stability of this material.

To obtain a better insight into the reaction at the pyrolysis process, FT-IR spectra were obtained for chemical precursors before, at and after pyrolysis progress.

Fig. 4 shows the FT-IR spectra for the GDC precursors before and after pyrolysis. In the spectrum of the precursors after drying in a vacuum oven at 30 °C, the peak at 2950 cm^{-1} represents the methylene ($-CH_2-$),
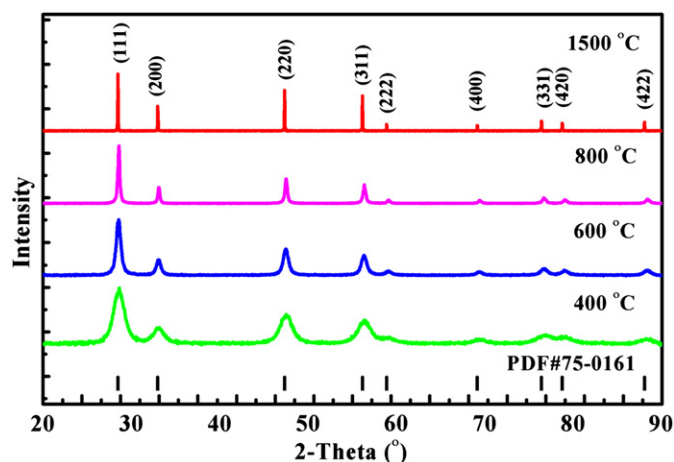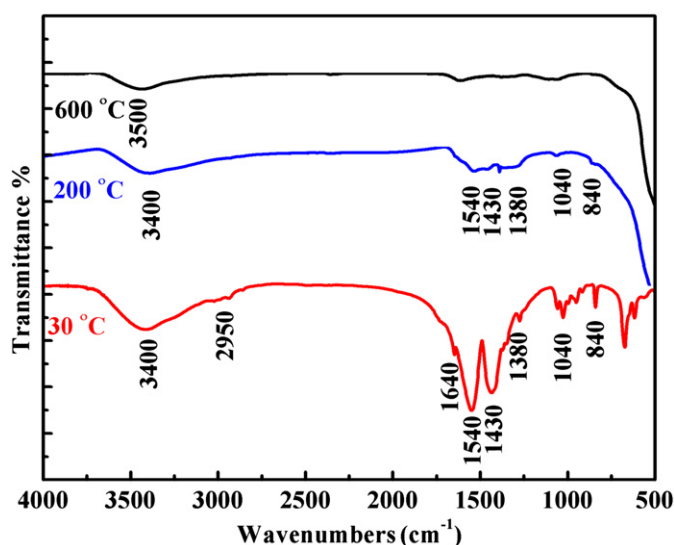

Fig. 4. FT-IR spectra of GDC precursors heat-treated at 30, 200 and 600 °C ($L/M=0.5$).

indicating the formation of PAA. What's more, a characteristic peak at 1640 cm^{-1} of AA is observed. This means that the AA was not completely polymerized, leaving a little to display a peak of the carbon–carbon double bond. Other vibrations are as follows: OH stretching (3400 cm^{-1}), CH_2 stretching (2920 cm^{-1}), C=O vibration (1540 cm^{-1}), COO^- vibration (1430 cm^{-1}), COO^- stretching (1380 cm^{-1}) and C–O stretching (1080 cm^{-1} and 1040 cm^{-1}).

It can be generally observed that after heating treatment there is a decrease in the intensity of those bands associated with carbon bonds. In the spectrum of the specimen dried at 200 °C, most of the infrared bands found in the dried precursor are observed. The C=O and C–O vibration ($\sim$1540 and 1430 cm^{-1}) can still be seen from the spectrum, indicating that the acetates did not fully decompose at this temperature. The broad and high absorption band at the range from 500 cm^{-1} to 700 cm^{-1} could be ascribed to metal–oxygen band, which indicates the formation of the GDC.

In the spectrum of GDC calcined at 600 °C, only the characteristic peaks of H_2O and the metal–oxygen band are observed. The presence of water is because of humidity in air. These acetate-related vibrations are no longer observed, indicating that the pyrolysis of organic compounds accomplished below 600 °C. Therefore the FT-IR spectra analysis result is in good agreement with TG/DTA and XRD results for the thermal decomposition process of the precursors as discussed above.

Then the influence of preparation conditions such as the molar ratio of acrylic acid to metallic ions (L/M) and the surfactant on the morphology and structure of the oxide particles has been studied. Firstly four kinds of GDC powders with $L/M = 0$, 0.5, 1, 4 were prepared and characterized by XRD and SEM. XRD results showed that all the samples are single cubic fluorite structure. The SEM morphologies of these GDC powders are shown in Fig. 5. It can be seen that the particles of the sample $L/M = 0$ were agglomerated and irregular, while the particles of samples $L/M = 0.5$, 1, 4 were similar, which were slightly agglomerated and near-spherical. So the application amount of acrylic acid were determined to be $L/M = 0.5$ in this study. However it can be calculated that the application amount of acrylic acid should be 8/3 in the classical polymer-pyrolysis method by the suggestion of Fu [12]. In order to explain this phenomenon, the FT-IR analysis was conducted below.

Fig. 6 shows the FT-IR spectra of the PAA, AA, the mix solution and the metal acetates. The L/M in the mix solution is 0.5 and the ratio of the cerium acetates to gadolinium acetates in the mix solution and the metal acetates is also the same with the preparation process. The

Curve a is the FT-IR spectrum of the poly (acrylic acid) (PAA) and the curve b is of the acrylic acid (AA), the monomer of PAA. Curve a is quite similar to Curve b, for PAA has a carbon–carbon single bond (C–C) and AA has a carbon–carbon double band (C=C). The characteristic peak of carbon–carbon double band at 1640 cm^{-1} is only observed in Curve b, and this is the most significant difference between AA and PAA. The broad band in the
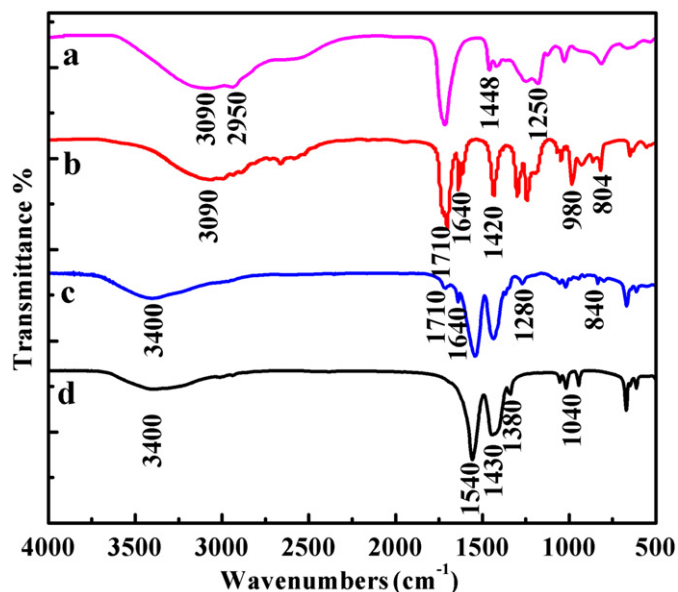

Fig. 6. FT-IR spectra of: (a) PAA, (b) AA, (c) AA and cerium and gadolinium acetates and (d) cerium and gadolinium acetates (molar ratio of acrylic acid to metallic ions is 0.5 and the ratio of cerium acetates to gadolinium acetates is stoichiometric).
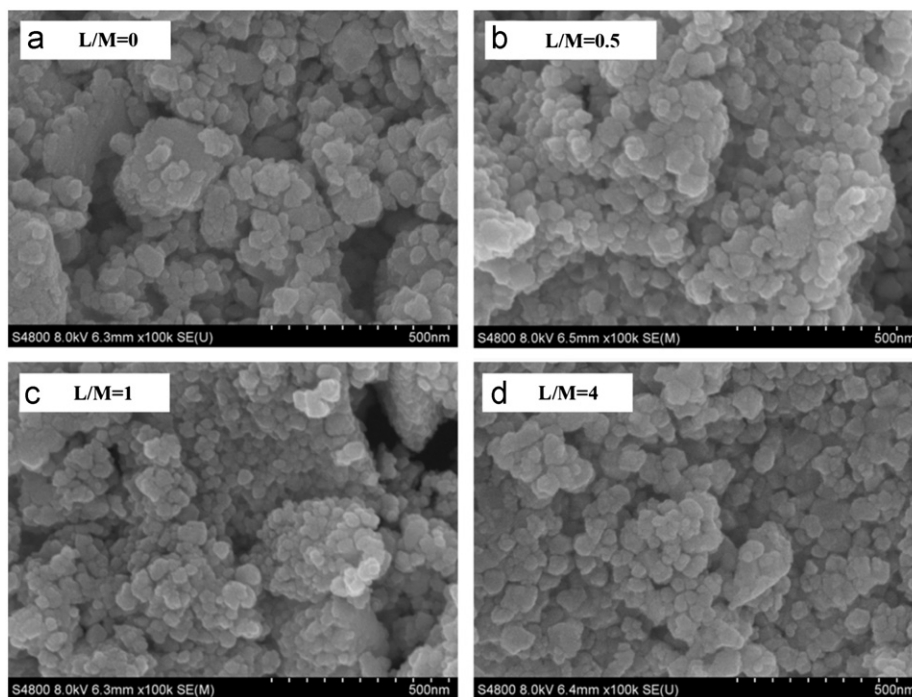

Fig. 5. SEM photographs of the GDC powders with different molar ratios of acrylic acid to metallic ions (L/M) of 0, 0.5, 1 and 4 calcined at 600 °C.

range of 3000–3700 cm^{-1} related to the presence of hydroxyl groups (O–H) is shown in Curves a and b because of the carboxyl groups in PAA and AA. The peak at 1710 cm^{-1} in both curves was attributed to carbonyl (C=O) vibration.

Curve C is assigned to the middle product when the metal acetates solution and acrylic acid mixed with the $L/M=0.5$ and Curve d represents the spectrum of the metal acetates solution which is the same with the preparation process. The Curves c and d are quite same except for the two peaks at 1710 cm^{-1} and 1640 cm^{-1}, which are the characteristic peaks of AA. The broad band at 3400 cm^{-1} was related to the presence of hydroxyl groups (O–H) because of the carboxyl groups in acetates. The band at about 1540 cm^{-1}, was attributed to carbonyl (C=O) vibration in the acetates, while the vibration and stretching of the carboxylate salts (COO)$^{-}$ were located at around 1430 cm^{-1} and 1380 cm^{-1}. The symmetric ($\sim$1080 cm^{-1}) and asymmetric ($\sim$1040 cm^{-1}) of C–O stretching can also be seen in Fig. 6c and d.

The 1710 cm^{-1} and 1640 cm^{-1} characteristic peaks are observed in Curve c, which means the existence of free AA in the mix solution. Another important feature in these spectra, when compared to AA, is the intensity ratio of bands at 1710 cm^{-1} and 1640 cm^{-1}. The increase in the intensity of the 1640 cm^{-1} band relative to that of the 1740 cm^{-1} band is attributed to the chemical bond between metallic cations and the AA. Parts of the carboxyl groups in AA complexed with the metallic ions and the peak shifted from 1710 cm^{-1} to about 1540 cm^{-1}.

The complexing ability to metallic ions of AA and PAA has some difference, which is due to the different molecular structure. The PAA only has a carbon–carbon single bond chain while the acrylic acid is an organic acid with conjugated double bond. The carbon–carbon double bond in AA conjugated with the double bond of carbon–oxygen double bond. This conjugated double bond leads to a delocalization effect on the whole molecule. This makes the electron density of the oxygen atom in the acrylic acid reduce. As a consequence of this delocalization effect, the complexing of the acrylic acid with the metal ions weakened when compared to the poly (acrylic acid).

The mix solution of AA and metal acetates was heated in an 80 °C water bath for 5 h and it turned into a gel. This is because the AA polymerized into PAA by thermal initiation. It is now well accepted that this polymerization reaction proceeds mainly through a free radical polymerization. The reaction of acrylate has been studied and discussed in detail by Fu [12]. They believed the polymerization reaction did not occur without the initiator. However, the band at 2950 cm^{-1} can be observed in the precursor, indicating the formation of the PAA. This proved that the free radical polymerization can be initiated by heating in water solution. The acrylic acid is an ideal monomer instead of acrylamide [11] for gel constitution. The low application amount and high effect of acrylic acid was attributed to the co-operation of carboxyl group and ethylenic bond.

On the other hand, it is well known that in soft chemical synthesis, surfactant addition also has an important effect on the solution and microstructure of the resultant. So another four kinds of GDC powders with $L/M=0.5$ and 0.5 g surfactants of polyvinyl alcohol (PVA), polyvinyl pyrrolidone (PVP), polyethylene glycol (PEG) and ethylene glycol (EG) respectively were prepared and characterized by
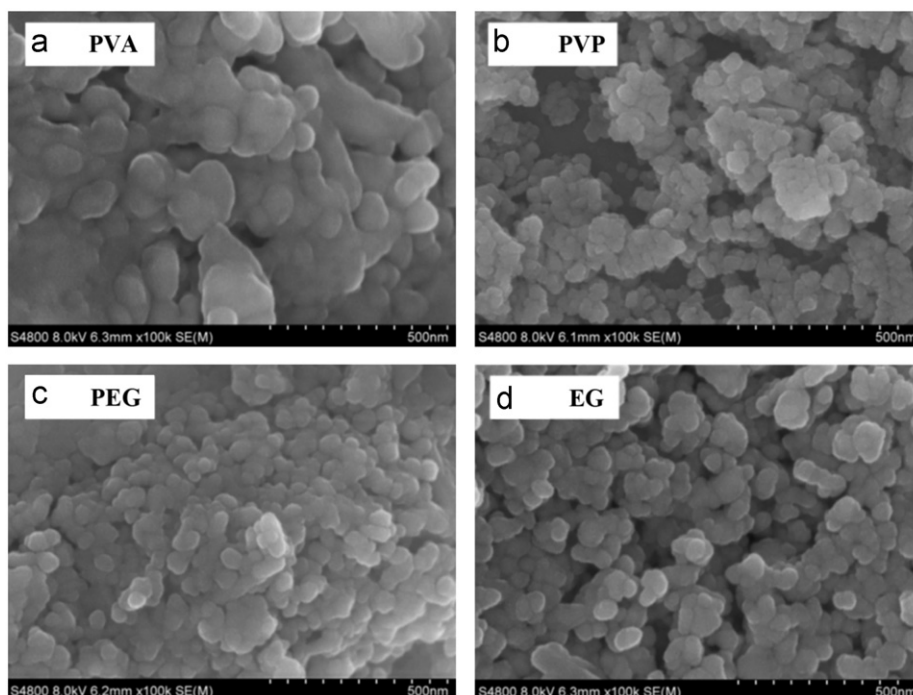

Fig. 7. SEM photographs of the GDC powders calcined at 600 °C with different surfactants (a) EG, (b) PEG, (c) PVA and (d) PVP ($L/M=0.5$).
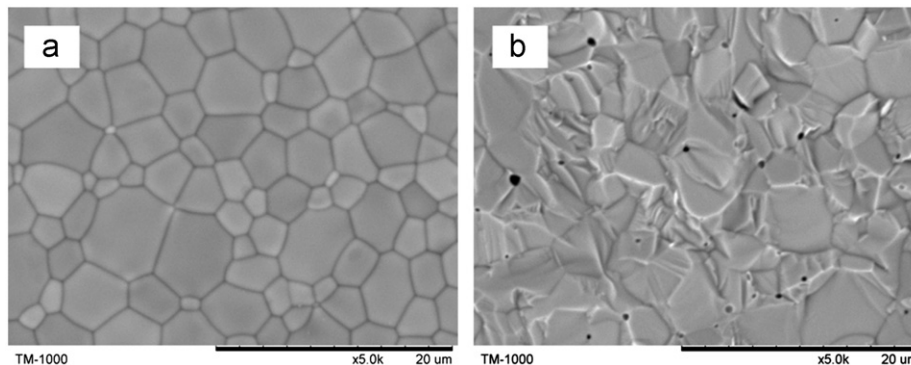
Fig. 8. SEM photographs of the surface (a) and fracture surface (b) of GDC pellet calcined at 1500 °C.

XRD and SEM. The XRD result shows that all the samples are single cubic fluorite structure. The SEM morphologies of these GDC powders are shown in Fig. 7. It is observed that in Fig. 7a the particles are tend to agglomerate rather than homogeneously distributed and the powder size are about 100 nm. The Fig. 7b has a smaller powder size of 50 nm but the particles are poorly distributed. The Fig. 7c has a better distribution compared to the Fig. 7b, but part of the particles agglomerated during the sintering process. The best morphology is achieved in Fig. 7d, which is well dispersed and has a particle size of 50 nm. As a result, EG was chosen to be the surfactant for the method.

As a whole, the optimization conditions of prepared the GDC powders are using acrylic acid as complexing and polymerization agent, $L/M = 0.5$, and EG as the surfactant. Furthermore, this preparation process was scaled up to a capacity of 2 kg powders per cycle, the GDC powders as-prepared were characterized by XRF, BET and PSD analysis. The XRF results show that the GDC powders are composed of CeO_2 89.2 wt% and Gd_2O_3 10.7 wt%, which indicates that the powders composition is near the nominal $Ce_{0.9}Gd_{0.1}O_{1.95}$, and the purity of the GDC powders is higher than 99.9%. The special surface area of the GDC powders is found to be 13.1 m^2g^{-1} at the calcination temperature of 600 °C. PSD analysis shows that the particle size of GDC powders is around 100–200 nm with a narrow distribution. In view of all characterizations of the GDC powders, it can be concluded that the process optimization has led a high purity, single phase, homogeneous and slight aggregation GDC powders with grain size 50 nm.

The resultant GDC powders were pressed into a pellet of 8 mm diameter and 1.0 mm thickness under a pressure of 300 MPa, and then calcined at 1500 °C for 5 h. The microstructures of the GDC ceramics are shown in Fig. 8. The Fig. 8a is the photograph of the pellet surface and the Fig. 8b is its fracture surface. It shows that the GDC pellet is nearly fully dense with very few residual pores. The well-developed grain boundary and the very low porosity are typical micro-structural features of a ceramic in the final stage of calcination. The calculated relative density for all samples is more than 99.0% of the theoretical value.
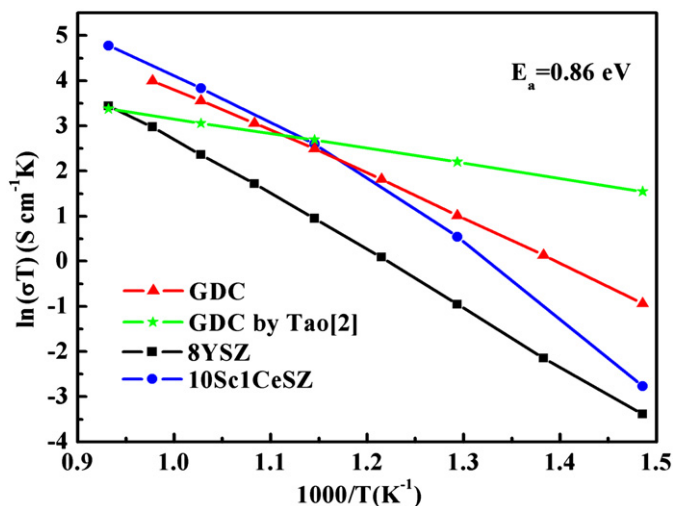

Fig. 9. Arrhenius plot of ionic conductivity of GDC, GDC in Tao [2], SSZ and YSZ.

The impedance of the material was measured from 400 °C to 800 °C for the dense pellets (>99.0%) of GDC, 8YSZ and 10Sc1CeSZ. The 8YSZ and 10Sc1CeSZ were synthesized by co-precipitation method[22]. The Arrhenius plot of the conductivity for these samples is shown in Fig. 9. The GDC sample shows a better conductivity than 8YSZ and it is comparable with 10Sc1CeSZ. The conductivity of the GDC sample, at 600, 650, 700, 750 °C is 0.014, 0.023, 0.036 and 0.053 Scm^{-1}. The dense GDC ceramic exhibits an ionic conductivity which is higher than Tao et al. [2] above 650 °C. The activation energy is 0.86 eV for the GDC ceramic in this work, which is larger than Tao's and in good agreement with the other reported values [10,20].

4. Conclusion

Nanocrystalline $Ce_{0.9}Gd_{0.1}O_{1.95}$ has been successfully synthesized via a simple acetic–acrylic method. The optimization conditions are using acrylic acid as complexing and polymerization agent, $L/M = 0.5$ and ethylene glycol as surfactant. This method is scaled up to a capacity of 2 kg powders per cycle. Process optimization has led a high purity, single phase, homogeneous and slight aggregation

GDC powders with grain size 50 nm. The AA played a significant role in the complexing of the metallic ions and the forming of the 3D network. The conductivity of the sintered $Ce_{0.9}Gd_{0.1}O_{1.95}$ sample is measured about 0.053 S cm^{-1} in air at 750 °C. These results have indicated that the acetic–acrylic method is an excellent technique to synthesize GDC powders with a good performance.

Acknowledgment

References

[1] Z. Gao, J. Huang, Z. Mao, C. Wang, Z. Liu, Preparation and characterization of nanocrystalline $Ce_{0.8}Sm_{0.2}O_{1.9}$ for low temperature solid oxide fuel cells based on composite electrolyte, International Journal of Hydrogen Energy 35 (2) (2010) 731–737.

[2] Y. Tao, J. Shao, J. Wang, W.G. Wang, Morphology control of $Ce_{0.9}Gd_{0.1}O_{1.95}$ nanopowder synthesized by sol–gel method using PVP as a surfactant, Journal of Alloys and Compounds 484 (1–2) (2009) 729–733.

[3] C. Viazzi, A. Deboni, J. Zoppas Ferreira, J.-P. Bonino, F. Ansart, Synthesis of Yttria Stabilized Zirconia by sol–gel route: influence of experimental parameters and large scale production, Solid State Sciences 8 (9) (2006) 1023–1028.

[4] C. Guizard, A. Julbe, O. Robbe, S. Sarrade, Synthesis and oxygen transport characteristics of dense and porous cerium/gadolinium oxide materials, Catalysis Today 104 (2–4) (2005) 120–125.

[5] D. Dong, Z. Chai, C.-Z. Li, H. Wang, Polymer hydrogel assisted combustion synthesis of highly crystalline ceramic nanoparticles for SOFC electrolyte films, Materials Chemistry and Physics 118 (1) (2009) 148–152.

[6] W. Chen, F. Li, J. Yu, Combustion synthesis and characterization of nanocrystalline CeO_2-based powders via ethylene glycol-nitrate process, Materials Letters 60 (1) (2006) 57–62.

[7] Y.P. Fu, C.H. Lin, C.S. Hsu, Preparation of ultrafine CeO_2 powders by microwave-induced combustion and precipitation, Journal of Alloys and Compounds 391 (1–2) (2005) 110–114.

[8] D.Y. Chung, E.H. Lee, Microwave-induced combustion synthesis of $Ce_{1-x}Sm_xO_{2-x/2}$ powder and its characterization, Journal of Alloys and Compounds 374 (1–2) (2004) 69–73.

[9] R. Peng, C. Xia, Q. Fu, G. Meng, D. Peng, Sintering and electrical properties of $(CeO_2)_{0.8}(Sm_2O_3)_{0.1}$ powders prepared by glycine–nitrate process, Materials Letters 56 (6) (2002) 1043–1047.

[10] A. Arabacı, M.F. Öksüzömer, Preparation and characterization of 10mol% Gd doped CeO_2 (GDC) electrolyte for SOFC applications, Ceramics International 38 (8) (2012) 6509–6515.

[11] A. Tarancón, G. Dezanneau, J. Arbiol, F. Peiró, J.R. Morante, Synthesis of nanocrystalline materials for SOFC applications by acrylamide polymerisation, Journal of Power Sources 118 (1–2) (2003) 256–264.

[12] X.M. Liu, G. Yang, S.Y. Fu, Mass synthesis of nanocrystalline spinel ferrites by a polymer-pyrolysis route, Materials Science and Engineering: C 27 (4) (2007) 750–755.

[13] J. Chandradass, B. Nam, K.H. Kim, Fine tuning of gadolinium doped ceria electrolyte nanoparticles via reverse microemulsion process, Colloids and Surfaces A: Physicochemical and Engineering Aspects 348 (1–3) (2009) 130–136.

[14] K. Nagy, I. Dékány, Preparation of nanosize cerium oxide particles in W/O microemulsions, Colloids and Surfaces A: Physicochemical and Engineering Aspects 345 (1–3) (2009) 31–40.

[15] Z. Gao, R. Raza, B. Zhu, Z. Mao, C. Wang, Z. Liu, Preparation and characterization of $Sm_{0.2}Ce_{0.8}O_{1.9}/Na_2CO_3$ nanocomposite electrolyte for low temperature solid oxide fuel cells, International Journal of Hydrogen Energy 36 (6) (2011) 3984–3988.

[16] E.C.C. Souza, E.N.S. Muccillo, Effect of solvent on physical properties of samaria-doped ceria prepared by homogeneous precipitation, Journal of Alloys and Compounds 473 (1–2) (2009) 560–566.

[17] T. Karaca, T.G. Altınçekiç, M. Faruk Öksüzömer, Synthesis of nanocrystalline samarium-doped CeO_2 (SDC) powders as a solid electrolyte by using a simple solvothermal route, Ceramics International 36 (3) (2010) 1101–1107.

[18] S. Dikmen, Effect of co-doping with Sm^{3+}, Bi^{3+}, La^{3+}, and Nd^{3+} on the electrochemical properties of hydrothermally prepared gadolinium-doped ceria ceramics, Journal of Alloys and Compounds 491 (1–2) (2010) 106–112.

[19] Z. Khakpour, A. Yuzbashi, A. Maghsodipour, K. Ahmadi, Electrical conductivity of Sm-doped CeO_2 electrolyte produced by two-step sintering, Solid State Ionics 227 (2012) 80–85.

[20] K. Maca, J. Cihlar, K. Castkova, O. Zmeskal, H. Hadraba, Sintering of gadolinia-doped ceria prepared by mechanochemical synthesis, Journal of the European Ceramic Society 27 (13–15) (2007) 4345–4348.

[21] A. Sin, P. Odier, Gelation by acrylamide, a quasi-universal medium for the synthesis of fine oxide powders for electroceramic applications, Advanced Materials 12 (9) (2000) 649–652.

[22] M. Liu, C. He, J. Wang, W.G. Wang, Z. Wang, Investigation of $(CeO_2)_x(Sc_2O_3)_{(0.11-x)}(ZrO_2)_{0.89}$ ($x=0.01–0.10$) electrolyte materials for intermediate temperature solid oxide fuel cell, Journal of Alloys and Compounds 502 (2) (2010) 319–323.